Open access • Posted Content • DOI:10.1101/2021.05.25.445649

Divergent early antibody responses define COVID-19 disease trajectories

Saborni Chakraborty, Joseph C. Gonzalez, Benjamin L. Sievers, Vamsee Mallajosyula ...+23 more authors

Institutions: Stanford University, J. Craig Venter Institute, San Jose State University, University of California, San Francisco ...+4 more institutions

Published on: 25 May 2021 - bioRxiv (Cold Spring Harbor Laboratory)

Topics: Neutralizing antibody and Antibody

Divergent early antibody responses define COVID-19 disease trajectories

Saborni Chakraborty[1]†, Joseph C. Gonzalez[1,2]†, Benjamin L. Sievers[3]†, Vamsee Mallajosyula[4], Megha Dubey[5], Bowie Yik-Ling Cheng[1], Kim Quyen Thi Tran[1], Srijoni Chakraborty[6], Arianna Cassidy[7], Steven T. Chen[8,9,10], Aanika Sinnott[16], Terri Gelbart [16], Yarden Golan[11], Mary Prahl[12], Upinder Singh[1,5], Seunghee Kim-Schulze[8], Robert Sherwood[13], Sheng Zhang[13], Thomas U. Marron[8], Sacha Gnjatic[8], Stephanie L. Gaw[7], Kari C. Nadeau[14], Miriam Merad[8,9,10,15], Prasanna Jagannathan[1,5], Gene S. Tan[3,16*], Taia T. Wang[1,5,17*]

[1]Department of Medicine, Division of Infectious Diseases, Stanford University, Stanford, CA, USA.

[2]Immunology Interdepartmental Program, Stanford University, Stanford, CA, USA.

[3]J. Craig Venter Institute, La Jolla, CA, USA.

[4]Institute for Immunity, Transplantation, and Infection, Stanford University School of Medicine, Stanford, CA, USA.

[5]Department of Microbiology and Immunology, Stanford University, Stanford, CA, USA.

[6]Department of Computer and Software Engineering, San Jose State University, San Jose, CA, USA.

[7]Division of Maternal-Fetal Medicine, Department of Obstetrics, Gynecology, and Reproductive Sciences, University of California San Francisco, CA, USA.

[8]The Precision Immunology Institute, Icahn School of Medicine at Mount Sinai, New York, NY, USA

[9]The Tisch Cancer Institute, Icahn School of Medicine at Mount Sinai, New York, NY, USA

[10]Department of Oncological Sciences, Icahn School of Medicine at Mount Sinai, New York, NY, USA

[11]Department of Bioengineering and Therapeutic Sciences, and Institute for Human Genetics, University of California, San Francisco, CA, USA.

[12]Division of Pediatric Infectious Diseases, Department of Pediatrics, University of California, San Francisco, CA, USA.

[13]Proteomics and Metabolomics Facility, Institute of Biotechnology, Cornell University, Ithaca, NY, USA.

[14]Sean N. Parker Center for Allergy and Asthma Research, Stanford, CA, USA.

[15]Human Immune Monitoring Center, Icahn School of Medicine at Mount Sinai, New York, NY, USA

[16]Division of Infectious Diseases, Department of Medicine, University of California San Diego, La Jolla, CA, USA.

[17]Chan Zuckerberg Biohub, San Francisco, CA, USA.

† these authors contributed equally

* these authors contributed equally

Corresponding author: taiawang@stanford.edu

Abstract:

Serologic markers that predict severe COVID-19 disease trajectories could enable early medical interventions and reduce morbidity and mortality. We found that distinct features of IgG Fab and Fc domain structures were present within three days of a positive test that predicted two separate disease trajectories in a prospective cohort of patients with COVID-19. One trajectory was defined by early production of neutralizing antibodies and led to mild disease. A distinct trajectory, characterized by an initial period of mild symptoms followed by rapid progression to more severe outcomes, was predicted by the absence of early neutralizing antibody responses with concomitant production of afucosylated IgGs. Elevated frequencies of monocytes expressing the receptor for afucosylated IgGs, FcγRIIIa (CD16a), were an additional antecedent in patients with the more severe outcomes. In mechanistic studies, afucosylated immune complexes in the lung triggered an inflammatory infiltrate and cytokine production that was dependent on CD16a. Finally, in healthy subjects, mRNA SARS-CoV-2 vaccination elicited neutralizing antibodies that were enriched for Fc fucosylation and sialylation and distinct from both infection-induced trajectories. These data show the importance of combined Fab and Fc domain functions in the antiviral response, define an early antibody signature in people who progressed to more severe COVID-19 outcomes and have implications for novel therapeutic strategies targeting FcγRIIIa pathways.

Introduction

IgG activities *in vivo* arise from combined actions mediated by the fragment antigen-binding (Fab) and fragment crystallizable (Fc) domains. Fab domains determine binding specificity and the ability of antibodies to block virus attachment to host cells while Fc-Fc gamma receptor (FcγR) interactions trigger a variety of effector cell functions. The structure of anti-viral Fab and Fc domains determines whether opsonized virus particles will be neutralized and how they will be engaged by host cells. COVID-19 is associated with a wide range of clinical outcomes and why most people experience mild or no symptoms while others progress to severe disease or death is not well understood. Further, how the kinetics and quality of the early antibody response impact the trajectory of COVID-19 is not fully known. Understanding the Fab and Fc domain structures that predict different COVID-19 disease trajectories would provide an opportunity for early medical interventions to reduce morbidity and mortality associated with this disease.

Post-translational modifications (PTMs) of the Fc are one of the major mechanisms by which Fc structure is regulated. Fc fucosylation and sialylation are tightly regulated PTMs that confer distinct and well-defined activities of IgG1 antibodies by governing their affinity to FcγRs expressed on innate immune cells[1,2]. Engagement of the FcγRs bearing innate immune cells, in turn, transduces the activities of IgGs into cell-mediated immune responses. Low levels of Fc fucosylation (afucosylation) have been observed in late COVID-19, a disease caused by severe acute respiratory syndrome coronavirus 2 (SARS-CoV-2), specifically in hospitalized patients with severe disease[3,4]. Yet, whether Fc afucosylation is a predictive marker of susceptibility to more severe COVID-19 is unknown. One well characterized phenotype within the spectrum of COVID-19 manifestations is mild symptoms lasting for several days followed by rapid progression to more severe symptoms that may require hospitalization[5,6]. This group is particularly important to study

as they present an opportunity to intervene to prevent morbidity and mortality associated with more severe COVID-19.

A role for antibodies in modulating COVID-19 severity has been suggested by several studies. Most studies have focused on the role of the Fab in binding and neutralization. Early administration of passively transferred neutralizing antibodies, for example, can protect from severe disease [7-10]. In addition, a delayed neutralizing response is associated with mortality in severe COVID-19 [11]. The afucosylated IgG antibodies that are enriched in patients with severe later-stage disease may also modulate disease[3,4]. This Fc modification, when incorporated into SARS-CoV-2 immune complexes, enhances affinity for FcγRIIIa/CD16a and can trigger numerous cellular effector functions, including production of inflammatory cytokines by primary monocytes, such as IL-6 and TNF [3]. Whether afucosylated antibodies in patients with severe COVID-19 are a response to severe infection or are antecedent to disease progression has not been clear. Here, we dissect the evolution of neutralizing and afucosylated antibody forms after SARS-CoV-2 infection. By tracing the early antibody signatures associated with distinct disease outcomes, we have been able to identify that early afucosylated antibodies together with low serum neutralizing activity are, in fact, an early predictor of more severe disease outcomes. We also show that two doses of mRNA vaccination elicit antibodies with protective signatures characterized by high neutralizing titers and elevated sialylation and low afucosylation of anti-S IgG Fc.

Results

Neutralizing antibody dynamics in a ten-month longitudinal cohort of COVID-19 outpatients. To gain an understanding of the kinetics of neutralizing antibody production in COVID-19 and any patterns of production that may be associated with specific disease

trajectories, we studied neutralizing antibodies over time in the longitudinal cohort of 109 COVID-19 outpatients from Stanford Hospital Center. These study participants were enrolled within three days of a positive SARS-CoV-2 PCR test. All subjects were assessed by a physician and had asymptomatic or mild COVID-19 at the time of enrollment. Because subjects in this study were enrolled within 3 days of a first positive SARS-CoV-2 PCR test, samples were drawn at an unusually early stage of disease (the median duration of symptoms prior to enrollment was 3 days; mean was 3.11 days) (Fig. 1A). Disease resolution occurred in most subjects, though the duration of symptoms was highly variable within the cohort (range 0-50 days). Though all subjects had mild COVID-19 at the time of the first sample draw, 8 subjects had acutely worsening symptoms in the hours or days following enrollment, leading to evaluation in the emergency department; five of these individuals ultimately required hospitalization. We term these individuals "progressors" (Table 1). Overall, this cohort enabled a granular prospective study of the evolution of the different antibody types early after infection in patients with distinct clinical outcomes. Of note, the original purpose of this prospective study was to assess whether interferon lambda could modulate the course of mild COVID-19; thus, study subjects were randomized to receive pegylated interferon lambda (lambda) or placebo after enrollment[12]. Administration of lambda had no effect on the clinical course of disease[12] and there was no correlation between the generation of neutralizing antibodies after infection and receipt of lambda (Extended Data Fig. 1). "Early" (study day 0) antibody responses that were characterized here were from samples obtained before subjects received either lambda or placebo treatment.

To define the evolution of the antibody response following exposure to SARS-CoV-2, we performed neutralization assays using a pseudotyped vesicular stomatitis virus system. The fifty percent pseudoviral neutralizing antibody titers (pNT_{50}) and IgG binding antibody titers were calculated at study day 0 (enrollment), day 5, day 28, month 7 and month 10 for all subjects from whom samples were available. Levels of both binding and neutralizing antibodies showed a

significant increase over time from day 0 and peaked at the day 28 timepoint (Fig. 1B). The longitudinal pNT_{50} for each study subject was evaluated by overall Symptom Day (Fig. 1B) and a majority of subjects were negative for neutralizing antibodies on study day 0 (Fig. 1C). Once initiated, the antibody response was durable and persisted in most people until 7 months post-enrollment, after which there was a general decrease in binding titer and in neutralization by month 10 . A graphical representation of the kinetics of neutralizing antibody titers is shown in Fig 1C.; this analysis revealed heterogeneity in early neutralizing responses within non-progressors, while progressors were uniformly negative for early neutralizing antibodies despite having measurable anti-S and, in some, anti-N IgG antibodies (Fig. 1D).

We next asked whether there were any qualitative differences in the Fc structures of the IgGs from progressors prior to actual symptom progression. As we have previously observed elevated anti-SARS-CoV-2 Fc afucosylation at a late time point in disease (hospitalization)[3] and also in this study in an independent cohort of 52 hospitalized patients from Mount Sinai Hospital, we sought to clarify whether this Fc modification might actually define people who were at high risk for disease progression at an early time point after infection. Indeed, progressors were distinguished by elevated afucosylated anti-SARS-CoV-2 IgG1 at study enrollment and prior to worsening of symptoms (Fig. 1E). The level of Fc afucosylation in progressors was similar to levels observed in the hospitalized patients from Mount Sinai Hospital (Fig 1E). Other Fc glycoforms were not distinct between progressors and other outpatients, demonstrating specificity of Fc afucosylation as a predictor of disease trajectory (Extended Data Fig. 2). Interestingly, the frequency of afucosylated anti-SARS-CoV-2 IgG1 was inversely correlated with pNT_{50} such that higher afucosylation was not present in people with high early neutralizing antibody responses (Fig. 1F).

We next trained and evaluated a random forest classifier by using early neutralization titers and afucosylation as input features to separate progressors and non-progressors. Individually, both

Fc afucosylation and early neutralization titers had modest predictive powers, while combining the two features could separate progressors from non-progressors with high predictive accuracy (Fig. 1G). Thus, early production of reactive, afucosylated antibodies and poor serum neutralizing activity predicted progression from mild COVID-19 to more severe outcomes (Table 1).

Elevated activating FcγR signaling potential in myeloid compartment of progressors. In addition to afucosylated antibody production, a hallmark of patients with severe COVID-19 is inflammatory myeloid cell infiltration into lungs and excessive inflammatory cytokine production [13-15]. These cells express the low affinity FcγRs FcγRIIa/CD32a (activating), FcγRIIb/CD32b (inhibitory) and, on some subsets, FcγRIIIa/CD16a (activating). These FcγRs are engaged through avidity-based interactions when immune complexes are formed during infection. Depending on the strength of activating and inhibitory signaling, effector cells respond with a proportional level of inflammatory activity[3]. Thus, we investigated whether there were any distinctions in FcγR expression on myeloid cells in subjects with distinct COVID-19 trajectories.

To study this, PBMCs collected at study enrollment were assessed for the frequency of different leukocyte subsets and we further quantified the expression of low affinity FcγRs by those subsets. Notably, we found that at study enrollment, progressors already had an increased frequency of CD16a+ monocytes in the peripheral blood compared to other outpatients (Fig. 2A). CD16a expression within the myeloid compartment, as a whole, was elevated in progressors, while other low affinity FcγRs were not distinct between progressors and non-progressors (Fig. 2B). The normalized co-expression of CD16a, CD32a, and CD32b revealed that myeloid cells from progressors exhibited a significantly heightened activating/inhibitory (A/I) FcγR signaling potential (Figure 2C). Significant differences in the distribution of FCGR3A allelic variants (F/F, F/V and V/V) were not observed between non-progressors and progressors (Extended Data Fig. 3). Overall, elevated frequencies of CD16a+ monocytes and a higher A/I signaling potential of

myeloid cells separated progressors and non-progressors. Thus, elevations in both the ligand (afucosylated antibodies) (Fig. 1E) and the cognate receptor (CD16a) (Fig. 2A) were correlates of a progressive COVID-19 trajectory.

Afucosylated immune complexes trigger inflammation in the lung *in vivo*. That progressive COVID-19 was heralded by production of poorly neutralizing, afucosylated IgGs prompted us to study whether afucosylated immune complexes modulate the cellular or cytokine milieu within the lung. In this pursuit, we used an in vivo model to study the response to different human immune complexes in the lung of mice that are fully humanized for FcγRs [16]. This model does not distinguish between neutralizing and non-neutralizing antibodies, but rather can be used to dissect FcγR pathways that mediate the response to polyclonal immune complexes. Mice were intratracheally administered immune complexes composed of purified, polyclonal anti-SARS-CoV-2 IgGs with trimeric SARS-CoV-2 spike protein. The polyclonal IgG pools were purified from COVID-19 patients with either elevated (>20%) or normal levels (<10%) IgG1 Fc afucosylation and were standardized for binding to SARS-CoV-2 spike. Four hours after administration, bronchoalveolar lavage (BAL) was performed and the collected fluid was promptly analyzed for immune cell and cytokine content. This time point was chosen based on established mouse models of immune complex mediated activities in the lung [12, 13].

BAL from mice that received afucosylated immune complexes was infiltrated by neutrophils and monocytes and this infiltration was dependent on CD16a (Fig. 3A). BAL fluid from mice that received afucosylated immune complexes was also distinguished from all other experimental conditions by the presence of the proinflammatory cytokines and chemokines TNFα, IL-6, CXCL1, CCL3, and CCL4 while no difference was observed in levels of the suppressive cytokine IL-10 (Fig. 3B). Taken together, polyclonal afucosylated immune complexes drove changes in the

cellular environment in the lung and production of specific cytokines and chemokines that are consistent with changes observed in severe COVID-19 [14,17-19].

Early robust neutralizing antibody production in "rapid resolvers". Next, we evaluated whether early production of neutralizing antibodies in non-progressors was associated with any COVID-19 trajectory. To study this, we performed a correlation analysis of neutralizing, binding IgG, or binding IgA titers from days 0, 5 or 28 against the time to resolution or total symptom days. Interestingly, the only correlation with duration of disease was between time to resolution and neutralizing antibody and IgA titers at the earliest time point, study day 0. Higher titers of neutralizing and binding antibodies on study day 0 were associated with rapid resolution of symptoms (in 0-7 days) (Fig.4A, B, C) and were positively correlated with levels of white blood cells (WBCs) and platelets (Extended Data Fig. 4). There was no difference in the number of days of symptoms prior to enrollment between the rapid resolvers (0-7 days of symptoms) and others (8+ days of symptoms) (Extended Data Fig. 5). Overall, these data showed that, while lack of serum neutralizing antibodies and a presence of reactive, afucosylated IgGs predicted symptom progression in mild COVID-19 (Fig. 1), early robust neutralizing antibody production was associated with rapid symptom resolution (Fig. 4).

SARS-CoV-2 mRNA vaccination elicits neutralizing antibodies with low Fc afucosylation

Finally, we sought to characterize the quality of antibodies produced by SARS-CoV2 mRNA vaccination. Antibodies elicited after 1 or 2 doses of either the Pfizer or Moderna SARS-CoV-2 vaccines in two separate cohorts (pregnant women or non-pregnant individuals) were studied. SARS-CoV-2 spike-binding IgG (AUC), IgA (AUC) and pNT_{50}s were characterized. There was a significant increase in IgG binding and in neutralizing titers by 21 days after the second vaccine dose (PD2) as compared to the response after dose 1 (PD1) in both cohorts (Fig. 5A). When compared to patients with COVID-19, IgG antibody titers and pNT_{50}s at PD1 were comparable to

those elicited by COVID-19 outpatients (study day 28 shown) in both the vaccine cohorts. The responses after two doses were comparable to hospitalized patients with COVID-19 and the non-pregnant cohort but pNT_{50}s were significantly lower in the pregnancy cohort at PD2 (Fig. 5A). The response to vaccine boost was observed to be greater within the pregnancy cohort when the boost was administered during the 3rd trimester when compared with the 2nd trimester (Extended Data Fig. 6). The durability of antibody responses in the non-pregnant cohort was also characterized 90 days (M3) after the first dose and a significant decrease in antibody binding and neutralization was observed at this time point (Fig. 5A). Vaccination elicited lower IgA titers in both the cohorts when compared with patients with COVID-19. In all, mRNA vaccination elicited robust neutralizing antibody responses, comparable to titers elicited in severe SARS-CoV-2 infections.

Over time, from post primary immunization (day 21) to 7 days post boost (day 28) and 3 weeks post boost (day 42), a subset of individuals had a clear elevation in IgG1 levels from day 21 to day 28 along with a decrease in IgG2. On evaluation of the kinetics of anti-SARS-CoV-2 Fc sialylation and afucosylation, no clear trends were observed (Fig. 5B, C); this contrasts with our observations after seasonal influenza virus vaccination, suggesting differences in the response that may be based on antigen experience or different vaccine platforms[20]. Interestingly, consistent with prior observations after seasonal influenza virus vaccination, the fold change in antigen-specific IgG Fc sialylation was a correlate of the quality of the vaccine response, with enhanced sialylation predicting a more robust neutralizing antibody response after vaccination (Fig. 5D)[20]. In the context of influenza virus vaccination, we have previously defined the role of Fc sialylation in maturation of higher affinity antibody responses in a CD23-dependent pathway[20]. Further studies are now warranted to define the role of sialylation in maturation of the SARS-CoV-2 vaccine response.

Anti-SARS-CoV2 Fc glycoforms elicited after two doses of mRNA vaccine were distinct from those elicited by infection. Of note, levels of Fc afucosylation were comparable to the mild COVID-19 cohort and were significantly reduced relative to hospitalized COVID-19. Interestingly, levels of Fc sialylation were significantly increased over both outpatient and hospitalized COVID-19 suggesting differential regulation of Fc sialylation in the context of mRNA vaccination and infection (Fig. 5E). Together, low afucosylation and elevated sialylation is consistent with modulatory IgG glycoforms that likely have a role in the maturation of the potent neutralizing response elicited by mRNA vaccines[20].

Discussion

Effective treatments that can prevent long term symptoms of COVID-19 or that may halt the progression to severe COVID-19 are urgently needed to prevent mortality in communities that have not yet benefited from vaccination. To identify new avenues of treatment, mechanisms underlying the distinct trajectories in COVID-19 must be clarified. Here, we show that there is a critical window of time in mild COVID-19 when antibody quality may be used to anticipate distinct COVID-19 trajectories, including progression to severe outcomes. We further show that progressors had elevated CD16a monocytes while still exhibiting mild COVID-19 symptoms. That both the afucosylated Fc ligand and the CD16a receptor were elevated in patients with mild COVID-19 who experienced a worsening disease trajectory over time suggests shows that this pathway is differentially regulated and enhanced in COVID-19 progressors and might be targeted for therapeutic purposes.

While the *in vivo* system used in experiments for this study is not a model of COVID-19 pathogenesis, it demonstrates that polyclonal afucosylated antibodies may form immune complexes with viral particles or antigens to promote an inflammatory environment in the lungs. Notably, the increased frequency of neutrophils and monocytes observed within the lungs of mice that received afucosylated immune complexes mirrors what has been observed in some severe patients with COVID-19[14,17-19]. Additional studies will be required to dissect which cells within the lung are the source of the factors that we observed in response to polyclonal afucosylated immune complexes. Alveolar macrophage (AMs) may have a central role as they are the predominant immune cell population within the lung under normal, unperturbed conditions, express high levels of FcγRIIIa/CD16a and can produce many of these specific factors in response to afucosylated immune complexes *ex vivo* [21].

An additional important topic for future studies is how Fc fucosylation is regulated and whether there are genetic and/or modifiable determinants of this post-translational modification. The distinctions in PTMs on IgGs elicited by SARS-CoV-2 infection and mRNA vaccination show differential regulation on the basis of the eliciting antigen but there are clearly additional determinants that cause some people to produce elevated levels of afucosylated IgGs while a majority of people do not. Overall, these data support the critical role of early neutralizing antibodies in protection against COVID-19 and show that more severe disease trajectories may be identified early, revealing an opportunity for therapeutic intervention.

Materials and Methods

Cell lines. Human embryonic kidney (HEK) 293T (American Type Culture Collection, ATCC; CRL-3216) and Vero (ATCC; CCL-81) cells were grown and maintained in 1X Dulbecco's Modified Eagle Medium (DMEM; ThermoFisher Scientific) supplemented with 10% fetal bovine serum (FBS).

Cloning, expression and protein purification. The His_6-tagged SARS-CoV-2 RBD and full length SARS-CoV-2 spike protein were purified in house as previously described.[3] Briefly, both the constructs were transiently transfected into Expi293F cells (Thermo Fisher Scientific) and proteins purified from culture supernatants Ni-nitriloacedic acid (NTA) resin (GE HealthCare).

ELISA. ELISA was performed following a modified version of a protocol described previously[3]. Briefly, 96 Well Half-Area microplates (Corning (Millipore Sigma)) plates were coated with antigens at 2μg/ml in PBS for 1h at room temperature (RT). Next, the plates were blocked for an hour with 3% non-fat milk in PBS with 0.1% Tween 20 (PBST). All serum samples from patients with COVID-19, and the negative controls were heated at 56°C for 1h, aliquoted and stored at -80°C. Sera were diluted fivefold starting at 1:50 in 1% non-fat milk in PBST. 25μl of the diluted sera was added to each well and incubated for 2h at RT. Following primary incubation with the sera, 25 μl of 1:5000 diluted horse radish peroxidase (HRP) conjugated anti-Human IgG and IgA secondary antibodies (Southern Biotech) were added and incubated for 1h at RT. The plates were developed by adding 25μl/well of the chromogenic substrate 3,3′,5,5′-tetramethylbenzidine (TMB) solution (Millipore Sigma). The reaction was stopped with 0.2N sulphuric acid (Sigma) and absorbance was measured at 450nm (iD5 SPECTRAmax, Molecular Devices). The plates were washed 5 times with PBST between each step and an additional wash with PBS was done before

developing the plates. All data were normalized between the same positive and negative controls and the binding AUC has been reported.

Generation of SARS-CoV-2 pseudoparticles. To generate vesicular stomatitis virus (VSV) pseudotyped with the S of SARS-CoV-2, we first constructed an expression plasmid encoding the Wuhan S. We did this by modifying a pCAGGS mammalian expression vector encoding the full-length Wuhan S and deleting its last 18 amino acids of the cytoplasmic domain, which we call pCAGGS-SΔ18. This reagent was produced under HHSN272201400008C and obtained through BEI Resources, NIAID, NIH: Vector pCAGGS containing the SARS-related coronavirus 2, Wuhan S, NR52310. To generate VSV pseudotyped with SARS-CoV-2 S, we first coated 6-well plates with 0.5 µg/mL poly-D-lysine (ThermoFisher, Cat. No. A3890401) for 1 to 2 hours at room temperature (RT). After poly-D-lysine treatment, plates were washed three times with sterile water and then seeded with 1.5e6 cells of HEK 293T per well. After 24 hours (h), cells were transfected with 1 µg of pCAGGS-SΔ18 per well using Lipofectamine 2000 transfection reagent (ThermoFisher, Cat. No., 11668019). Forty-eight h after transfection, the cells were washed once with 1X phosphate buffered saline (PBS), and were infected with VSV-ΔG-GFP/nanoluciferase (a generous gift from Matthias J. Schnell) at a multiplicity of infection of 2 to 3 in a 300 µL volume. Cells were infected for an hour with intermittent rocking every 15 minutes. After infection, the inoculum was carefully removed, and the cell monolayer was washed three times with 1X PBS to remove residual VSV-ΔG-GFP/nanoluciferase. Two mL of infection media (2% FBS, 1% glutamine, 1% sodium pyruvate in 1X DMEM) was added to each well. At 24 h post-infection, the supernatants from all the wells were combined, centrifuged (600 *g* for 10 min, 4ºC), and stored at -80ºC until use.

Neutralization assays. Vero cells were seeded at 5e5 cells per well in 50 µL aliquots in half area Greiner 96-well plates (Greiner Bio-One; Cat. No. 675090) 24 h prior to performing the neutralization assay. On separate U-bottom plates, patient plasma was plated in duplicates and serially 5-fold diluted in infection media (2% FBS, 1% glutamine, 1% sodium pyruvate in 1X DMEM) for a final volume of 28 µL per well. We also included 'virus only' and 'media only' controls. Twenty-five microliters of SARS-CoV-2 pseudo-typed VSV particles (containing 500 to 1500 fluorescent forming units) were added to the wells on the dilution plate, not including the "virus-free" column of wells, and incubated at 37ºC for 1 hour. Prior to infection, Vero cells were washed twice with 1X PBS and then 50 µL of the incubated pseudo-typed particles and patient plasma mixture was then transferred from the U-bottom 96-well dilution plates onto the Vero cells and placed into an incubator at 37ºC and 5% CO2. At 24 h post-incubation, the number of GFP-expressing cells indicating viral infection were quantified using a Celigo Image Cytometer. We first calculate percent infection based on our 'virus only' controls and then calculate percent inhibition by subtracting the percent infection from 100. A non-linear curve and the half-maximal neutralization titer (NT50) were generated using GraphPad Prism.

Immune cell phenotyping and FcγR quantification. Cryopreserved human PBMCs were rapidly thawed, washed, and blocked with Human TruStain FcX (BioLegend) to reduce nonspecific binding. Cells were then stained for viability with Live/Dead Fixable Staining Kit (ThermoFisher) as well as the following antibody cocktail: anti-CD3 (BioLegend; clone OKT3), anti-CD11c (BioLegend; clone S-HCL-3), anti-CD14 (BioLegend; clone M5E2), anti-CD16 (BioLegend; clone 3G8), anti-CD19 (BioLegend; clone SJ25C1), anti-CD32 (STEMCELL; clone IV.3), anti-CD32B/C (BioLegend; clone S18005H), anti-CD56 (BioLegend; 5.1H11), and anti-HLA-DR (BioLegend; clone L243). After staining, cells were fixed and acquired using an Attune NxT flow cytometer (Invitrogen). Bulk myeloid cells were defined as viable CD3- CD19- CD56-

CD11c+ HLA-DR+ cells, while CD16a+ monocytes within this population were additionally positive for CD16a (Extended Data fig 7). Leukocyte expression of FcγRs was quantified by measuring the median fluorescence intensity (MFI) of a particular FcγR and comparing it to the MFI of stained Quantum™ Simply Cellular microsphere beads (Bangs Laboratories) of known and discrete antibody-binding capacities. A/I ratio was calculated by first applying range normalization to CD16a, CD32a, and CD32b expression. A/I ratio was calculated by the multiplication of range normalized CD16a and CD32a divided by CD32b. The resulting product was determined to correlate significantly with all inputs.

Determination of FCGR3A variants. Total RNA was extracted from PBMC samples using RNeasy Mini Kit (Qiagen, Cat no. 74104) and reverse transcribed into cDNA using SuperScript II Reverse Transcriptase Kit (ThermoFisher, Cat no. 18064022). PCR was performed to amplify FCGR3A gene using NEB Q5 Polymerase (New England BioLabs, Cat no. M0491L) and FCGR3A specific primers: 5'-TACAGGGTGCTCGAGAAGGACAGT-3' and 3'-TCTGTTCACTTAGCAACTTGGGA-5'. FCGR3A PCR products were purified using Monarch PCR & DNA Cleanup Kit (New England BioLabs, Cat no. T1030L) and subjected to Sanger sequencing using FCGR3A sequencing primer 5'- CATTGACGCTGCCACAGT-3'. The F/F, F/V and V/V variants of FCGR3A were determined by the ratio of G/T nucleotide based on the electropherograms from the Sanger sequencing result at the rs396991 SNP location. RNA extraction, reverse transcription, PCR and DNA purification were all performed per manufacturer's instruction.

***In vivo* lung inflammation.** All *in vivo* experiments were performed in compliance with federal laws and institutional guidelines and have been approved by the Stanford University Institutional Animal Care and Use Committee. Polyclonal IgG was isolated from PCR-positive SARS-CoV-2 patients' plasma, pooled based on the frequency of afucosylated anti-RBD IgG1 (>20% or <10%),

and incubated with SARS-CoV-2 spike trimer at a 20:1 molar ratio overnight at 4°C. Immune complexes were intratracheally administered to 8–12-week-old humanized FcγR or CD16a-deficient mice. 4hr post-administration, mice were sacrificed and bronchoalveolar lavage (BAL) was performed. Immune cells were isolated from within the BAL fluid and stained with the following cell staining panel: Live/Dead Fixable Dye (ThermoFisher), anti-CD2 (BioLegend; clone RM2-5), anti-CD3 (BioLegend; clone 17A2), CD11b (BioLegend; clone M1/70), anti-CD45 (BioLegend; clone I3/2.3), anti-human CD64 (BioLegend; clone 10.1), anti-B220 (BioLegend), anti- anti-Ly6G (BioLegend; clone 1A8), anti-MERTK (BioLegend; clone 2B10C42), anti-MHC II (BioLegend; clone M5/114.15.2). Once stained, cells were fixed and acquired via an Attune NxT flow cytometer (Invitrogen). Neutrophils were defined as viable Ly6G+ CD11b+ CD3- B220- leukocytes. Monocytes were defined as viable CD11b+ Ly6G- MERTK- MHC IA/IE- CD3- B220- leukocytes (Extended Data Fig 8). Cell-free BAL fluid was stored at 4°C and processed within 24hr to measure cytokine/chemokine content using a LEGENDplex bead array kit (BioLegend).

Clinical cohorts and samples

Characterization of these samples was performed under a protocol approved by the Institutional Review Board of Stanford University (protocol #55718).

Stanford Lambda cohort:

Longitudinal samples from 109 SARS-CoV-2-infected outpatients were obtained from a phase 2 randomized controlled trial of Peginterferon Lambda-1a (Lambda, NCT04331899). Inclusion/exclusion criteria and the study protocol for the trial have been published[12]. Briefly, adults aged 18-75 years with an FDA emergency use authorized reverse transcription-polymerase chain reaction (RT-PCR) positive for SARS-CoV-2 within 72 hours prior to enrollment

were eligible for study participation. Exclusion criteria included hospitalization, respiratory rate >20 breaths per minute, room air oxygen saturation <94%, pregnancy or breastfeeding, decompensated liver disease, recent use of investigational and/or immunomodulatory agents for treatment of COVID-19, and prespecified lab abnormalities. All participants gave written informed consent, and all study procedures were approved by the Institutional Review Board of Stanford University (IRB-55619). The median age of participants in this clinical trial was 36 years; 42% of participants were female, and 62.5% LatinX ethnicity. At enrollment, participants completed a standardized history, symptom questionnaire, physical exam and bloodwork. Participants were randomized 1:1 to receive a single subcutaneous injection of Lambda or saline placebo and followed for 28 days with a daily symptom survey (REDCap Cloud). Eight in-person visits were conducted post-enrollment with assessment of symptoms and vitals, and collection of oropharyngeal swabs for detection of SARS-CoV-2 RNA. Peripheral blood was collected at enrollment, day 5, and day 28 post enrollment. A subset of participants (n=80) returned for long-term follow-up visits 4,7, and 10 months post enrollment, with peripheral blood obtained.

Mount Sinai Cohort:

Sixty-one samples were obtained from hospitalized COVID-19 patients enrolled in the Mount Sinai Health System (MSHS) collected by the Mount Sinai COVID-19 biobank [22]. The median age was 65 years old with a range from 33 - 98 years old. There are 36 males and 25 females in the study. 13 patients succumbed to disease.

Stanford Adult vaccine cohort:

Fifty-seven healthy volunteers were enrolled in the study approved by Stanford University Institutional Review Board (IRB 8269). The median age was 36 years old with a range from 19 -

79 years old. There are 28 males and 29 females in the study. There are 27 White participants, 23 Asian participants, 4 Black participants, 1 Native American participant, and 2 other participants.

Pregnant vaccine cohort:

Fifty-eight female pregnant volunteers that received either the Moderna or Pfizer vaccine were enrolled in a study approved by the University of California at San Francisco Institutional Review Board (20-32077). Plasma samples were collected up to 24 hours before first vaccine dose, up to 24 hours before second dose, and 4-8 weeks after second vaccine dose. Additional opportunistic samples were collected at the time of routine blood draws and/or admission to labor and delivery. The median age at enrollment was 35 years old (range 27-42). The median gestational age was 21.5 weeks (range 5 to 40).

IgG Fc glycan analysis. Methods for relative quantification of Fc glycans and IgG subclasses have been previously described[20,23]. Briefly, IgGs were isolated from serum by protein G purification. Antigen-specific IgGs were isolated on NHS agarose resin (ThermoFisher; 26196) coupled to the protein of interest. Following tryptic digestion of purified IgG bound to antigen-coated beads, nanoLC-MS/MS analysis for characterization of glycosylation sites was performed on an UltiMate3000 nanoLC (Dionex) coupled with a hybrid triple quadrupole linear ion trap mass spectrometer, the 4000 Q Trap (SCIEX). MS data acquisition was performed using Analyst 1.6.1 software (SCIEX) for precursor ion scan triggered information dependent acquisition (IDA) analysis for initial discovery-based identification.

For quantitative analysis of the glycoforms at the N297 site of IgG1, multiple-reaction monitoring (MRM) analysis for selected target glycopeptide was applied using the nanoLC-4000 Q Trap platform to the samples which had been digested with trypsin. The m/z of 4-charged ions for all different glycoforms as Q1 and the fragment ion at m/z 366.1 as Q3 for each of transition pairs

were used for MRM assays. A native IgGs tryptic peptide (131-GTLVTVSSASTK-142) with transition pair of, 575.9^{+2}/780.4 was used as a reference peptide for normalization. IgG subclass distribution was quantitatively determined by nanoLC-MRM analysis of tryptic peptides following removal of glycans from purified IgGs with PNGase F. Here the m/z value of fragment ions for monitoring transition pairs was always larger than that of their precursor ions with multiple charges to enhance the selectivity for unmodified targeted peptides and the reference peptide. All raw MRM data was processed using MultiQuant 2.1.1 (SCIEX). All MRM peak areas were automatically integrated and inspected manually. In the case where the automatic peak integration by MultiQuant failed, manual integration was performed using the MultiQuant software.

Data and Statistical analysis. The log10 transformed half-maximal serum neutralization titers (pNT50) were used to generate the heatmap to show the evolution of antibody responses in longitudinal samples collected at different time-points after COVID-19 disease symptom onset. The data was clustered according to the serum neutralization titer kinetics.

The correlation and significance levels between any given pair of variables was computed using the rcorr() function in R 1.2.1335 using the Hmisc package and visualized using the corrplot package.

Python version 3.8.5 was used for machine learning. The output class progressor was mapped to 1 and non-progressor was mapped to 0, making it a binary classification problem. For the classification task, Random Forest Classifier was used. The input data was split using 6-fold cross validation in which the classifier was trained on 5 folds of the data and tested on the remaining part of the data. The ROC response for all these different datasets were used for calculating the mean area under curve.

All other data were analyzed with GraphPad Prism 9.0 software.

Acknowledgments: We thank Stanford CTRU Biobank, Catherine A. Blish, Hector Bonilla, Karen Jacobson, Diego Martinez Mori, Kattria van der Ploeg, Sharon Chinthrajah, Tina Sindher, Will Collins, James Liu, Joe G, Anthony Buccanco, Katia Tkachenko, Mihir Shah, Allie Lee, Kathleen Jia, Eric Smith, Iris Chang, Evan Do and Diane Dunham for support with clinical protocol, patient care, and/or collection/provision of patient samples.

Funding: Support was received from Stanford University, the Chan Zuckerberg Biohub, Prebys Foundation and the Searle Scholars Program. Research reported in this publication was supported by Fast Grants, CEND COVID Catalyst Fund, the Crown Foundation, the Sunshine Foundation, the Marino Family Foundation, the National Institute of Allergy and Infectious Diseases of the National Institutes of Health under Award Numbers U19AI111825, U54CA260517 and R01AI139119. S.G. and M.M were supported by NCI U24 grant CA224319. S.G. is additionally supported by grant U01 DK124165. M.M was supported by the fast-grant fund. S.G. reports consultancy and/or advisory roles for Merck and OncoMed and research funding from Bristol-Myers Squibb, Genentech, Celgene, Janssen R&D, Takeda, and Regeneron. The content is solely the responsibility of the authors and does not necessarily represent the official views of the National Institutes of Health.

Author contributions:

SC, JG, BLS, GST, TTW designed the study and analyzed data. SC, JG, GST, TTW wrote the manuscript with input from KN, TUM, PJ and VM. SC, JG, BLS, GST, VM, MD, BY-LC, KQTT, SC, RS, SZ performed experiments. AC, SC, TG, YG, SK, TUM, MP, US, AS, SLG, KN, SG, MM, PJ provided critical support and/or reagents.

Competing Interests: None

Additional information

Supplementary information

Correspondence and requests for materials should be addressed to T.T.W

Data availability

All raw data are available in the manuscript or from the corresponding author on request.

References

1 Wang, T. T. & Ravetch, J. V. Functional diversification of IgGs through Fc glycosylation. *The Journal of clinical investigation* **129**, 3492-3498, doi:10.1172/JCI130029 (2019).

2 Wang, T. T. IgG Fc Glycosylation in Human Immunity. *Current topics in microbiology and immunology*, doi:10.1007/82_2019_152 (2019).

3 Chakraborty, S. *et al.* Proinflammatory IgG Fc structures in patients with severe COVID-19. *Nat Immunol* **22**, 67-73, doi:10.1038/s41590-020-00828-7 (2021).

4 Larsen, M. D. *et al.* Afucosylated IgG characterizes enveloped viral responses and correlates with COVID-19 severity. *Science* **371**, doi:10.1126/science.abc8378 (2021).

5 Chang, M. C., Park, Y. K., Kim, B. O. & Park, D. Risk factors for disease progression in COVID-19 patients. *BMC Infect Dis* **20**, 445, doi:10.1186/s12879-020-05144-x (2020).

6 Mathew, D. *et al.* Deep immune profiling of COVID-19 patients reveals distinct immunotypes with therapeutic implications. *Science* **369**, doi:10.1126/science.abc8511 (2020).

7 Libster, R. *et al.* Early High-Titer Plasma Therapy to Prevent Severe Covid-19 in Older Adults. *The New England journal of medicine* **384**, 610-618, doi:10.1056/NEJMoa2033700 (2021).

8 Chen, P. *et al.* SARS-CoV-2 Neutralizing Antibody LY-CoV555 in Outpatients with Covid-19. *The New England journal of medicine* **384**, 229-237, doi:10.1056/NEJMoa2029849 (2021).

9 Weinreich, D. M. *et al.* REGN-COV2, a Neutralizing Antibody Cocktail, in Outpatients with Covid-19. *The New England journal of medicine* **384**, 238-251, doi:10.1056/NEJMoa2035002 (2021).

10 Schafer, A. *et al.* Antibody potency, effector function, and combinations in protection and therapy for SARS-CoV-2 infection in vivo. *The Journal of experimental medicine* **218**, doi:10.1084/jem.20201993 (2021).

11 Lucas, C. *et al.* Delayed production of neutralizing antibodies correlates with fatal COVID-19. *Nat Med*, doi:10.1038/s41591-021-01355-0 (2021).

12 Jagannathan, P. *et al.* Peginterferon Lambda-1a for treatment of outpatients with uncomplicated COVID-19: a randomized placebo-controlled trial. *Nat Commun* **12**, 1967, doi:10.1038/s41467-021-22177-1 (2021).

13 Del Valle, D. M. *et al.* An inflammatory cytokine signature predicts COVID-19 severity and survival. *Nature medicine* **26**, 1636-1643, doi:10.1038/s41591-020-1051-9 (2020).

14 Liao, M. *et al.* Single-cell landscape of bronchoalveolar immune cells in patients with COVID-19. *Nat Med* **26**, 842-844, doi:10.1038/s41591-020-0901-9 (2020).

15 Rendeiro, A. F. *et al.* The spatial landscape of lung pathology during COVID-19 progression. *Nature*, doi:10.1038/s41586-021-03475-6 (2021).

16 Smith, P., DiLillo, D. J., Bournazos, S., Li, F. & Ravetch, J. V. Mouse model recapitulating human Fcgamma receptor structural and functional diversity. *Proceedings of the National Academy of Sciences of the United States of America* **109**, 6181-6186, doi:10.1073/pnas.1203954109 (2012).

17 Schurink, B. *et al.* Viral presence and immunopathology in patients with lethal COVID-19: a prospective autopsy cohort study. *Lancet Microbe* **1**, e290-e299, doi:10.1016/S2666-5247(20)30144-0 (2020).

18 Nathan, C. Neutrophils and COVID-19: Nots, NETs, and knots. *J Exp Med* **217**, doi:10.1084/jem.20201439 (2020).

19 Sanchez-Cerrillo, I. *et al.* COVID-19 severity associates with pulmonary redistribution of CD1c+ DCs and inflammatory transitional and nonclassical monocytes. *J Clin Invest* **130**, 6290-6300, doi:10.1172/JCI140335 (2020).

20 Wang, T. T. *et al.* Anti-HA Glycoforms Drive B Cell Affinity Selection and Determine Influenza Vaccine Efficacy. *Cell* **162**, 160-169, doi:10.1016/j.cell.2015.06.026 (2015).

21 High titers and low fucosylation of early human anti-SARS-CoV-2 IgG promote inflammation by alveolar macrophages. *Sci Transl Med*, doi:10.1126/scitranslmed.abf8654 (2021).

22 Charney, A. W. *et al.* Sampling the host response to SARS-CoV-2 in hospitals under siege. *Nat Med* **26**, 1157-1158, doi:10.1038/s41591-020-1004-3 (2020).

23 Wang, T. T. *et al.* IgG antibodies to dengue enhanced for FcgammaRIIIA binding determine disease severity. *Science* **355**, 395-398, doi:10.1126/science.aai8128 (2017).

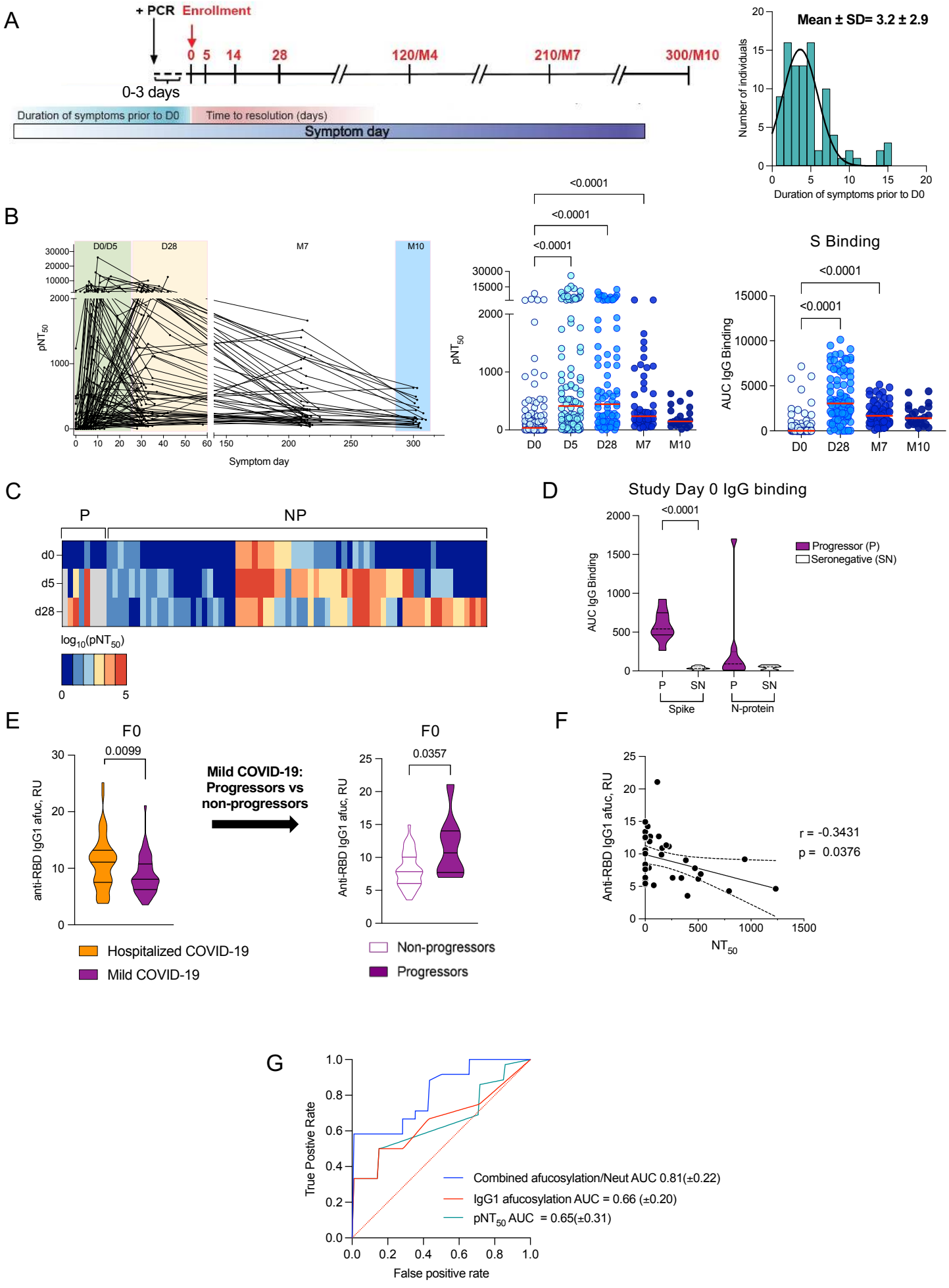

Figure 1. Low early neutralizing titers and elevated Fc afucosylation predict disease progression. (A) Longitudinal COVID-19 study timepoints, cohort characteristics and distribution of duration of symptoms in participants prior to enrolment. **(B)** The kinetics of neutralizing antibody response over time. Half-maximal SARS-CoV-2 pseudovirus neutralizing titers (pNT_{50}) and SARS-CoV-2 full length spike (S) binding IgG (AUC) at each time point ((D0, enrollment, n=109), day 5 (D5 n=108), day 28 (D28, n=92), month 7 (M7, n=65) and month 10 (M10, n=23)). The median values have been depicted with a red line. **(C)** Heatmap of longitudinal pNT_{50} data clustered according to the serum neutralization titer kinetics in progressors (P, n=8) and non-progressors (NP, n=68). **(D)** SARS-CoV-2 S and N-protein binding IgG (AUC) of progressors and seronegative (SN) historic sera samples. **(E)** Anti-RBD IgG1 Fc afucosylation (afuc/F0) in patients who were hospitalized (n=52) and in those who were seropositive upon study enrollment in the longitudinal outpatient cohort (n=49). Pre-progression (at study enrollment) IgG1 Fc afucosylation levels in progressors (n=8) and non-progressors (n=41). **(F)** The correlation between SARS-CoV-2 IgG1 afucosylation and D0 neutralization titers. (Pearson's correlation coefficient r=-0.3431, p=0.0376). **(G)** Mean ROC response and the area under the curve (AUC) with its standard deviation obtained using random forest classifier with 6-fold cross validation. P values (B) were calculated using Kruskal Wallis test with Dunn's correction and in (D, E) using unpaired students t test.

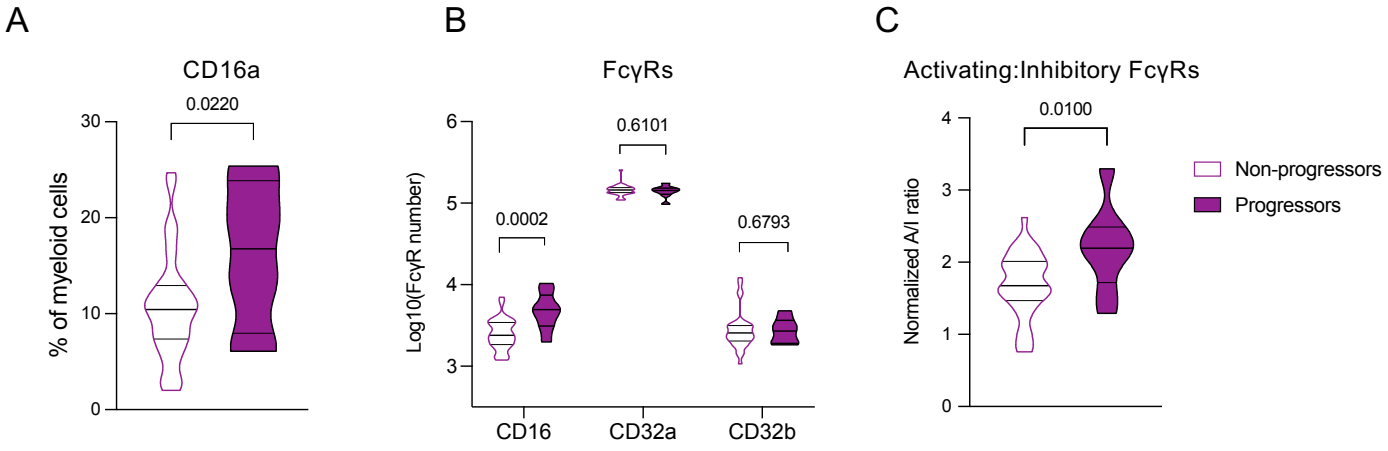

Figure 2. Elevated activating FcγR signaling potential in myeloid compartment of progressors Enrollment time point cells were characterized in progressors (n=8) and non-progressors (n=34). **(A)** CD16a+ monocyte frequencies as a percent of total CD11c+ HLA-DR+ lin- myeloid cells are shown. (**B**) Fcγ receptor (FcγR) expression on bulk myeloid cells in progressors as compared to non-progressors. **(C)** The activating to inhibitory ratio (A/I) which was calculated by combining the range normalized, quantitative expression of FcγRs CD16a, CD32a and CD32b. P values in (A-C) were calculated with unpaired students t test.

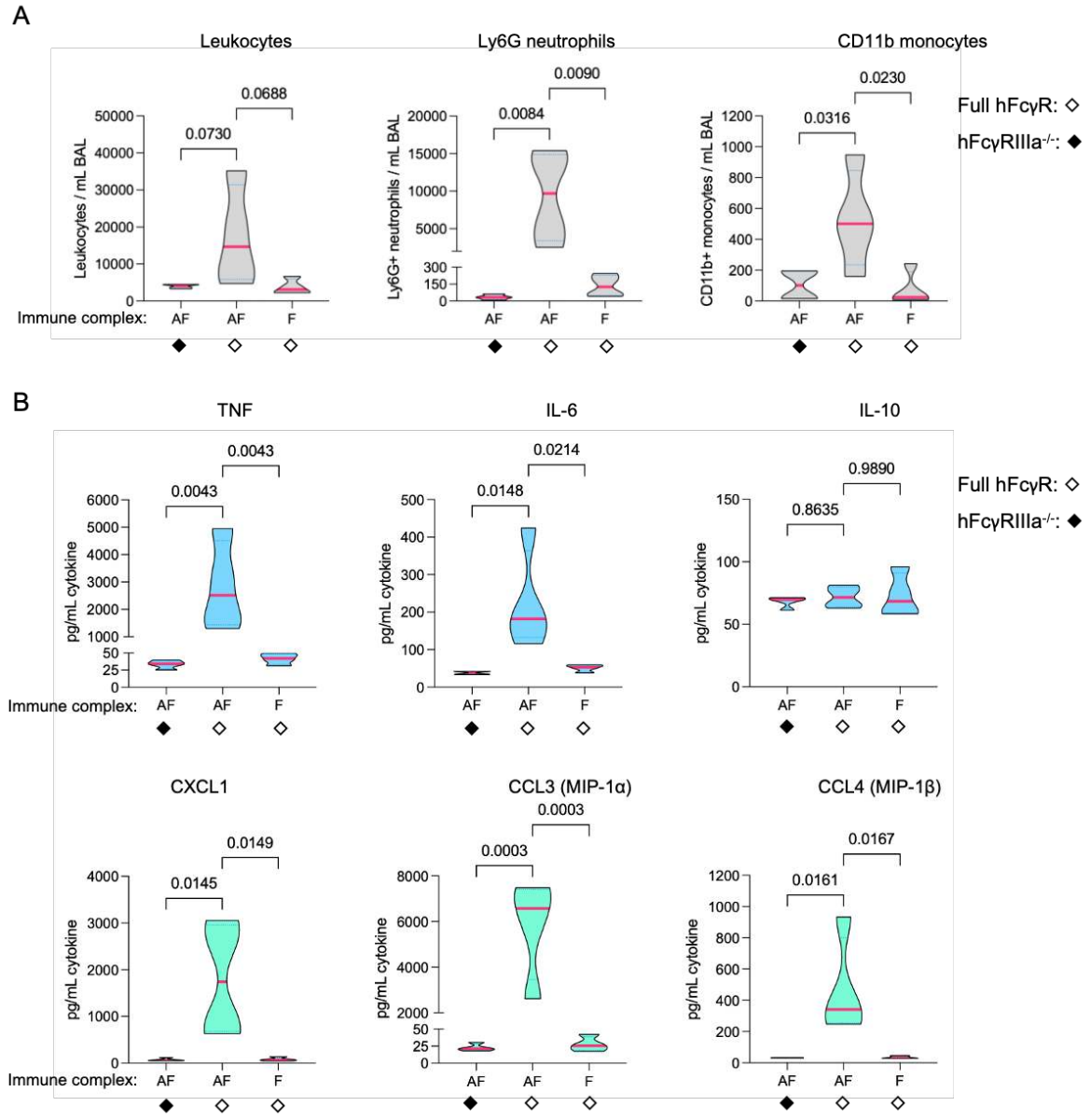

Figure 3. Afucosylated IgG immune complexes promote cell infiltration and proinflammatory cytokine production *in vivo*. (A) Immune cell subsets and **(B)** Cytokines/chemokines (TNF, IL-6, IL-10, CXCL1, CCL3, CCL4) quantitated in the bronchoalveolar lavage (BAL) fluid. Total leukocytes were defined as CD45+ cells, neutrophils were defined as Ly6G+ CD11b+ CD2- CD3- BV220- cells, total monocytes defined as CD11b+ Ly6G- MERTK- MHC IA/IE- CD2- CD3- BV220- cells. P values in A and B were calculated with one-way ANOVA using n=4 mice per group. Data in A are representative of two independent experiments.

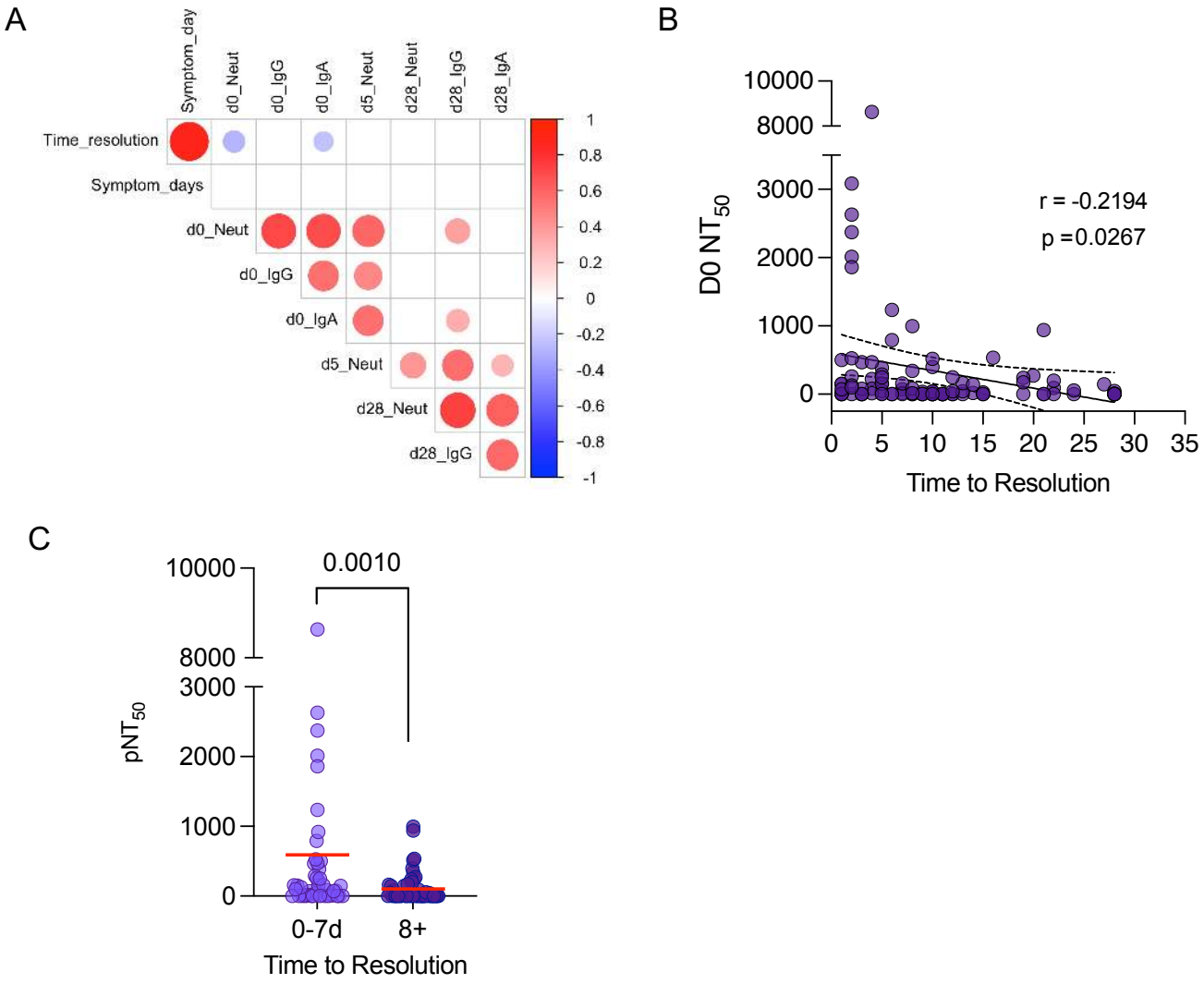

Figure 4. Early high neutralizing titers correlate with a shorter course of disease in non-progressors. (A) The cross-correlation matrix shows the relationship between multiple features of the antibody response (D0, D5 and D28 $pNT_{50,}$ D0 and D28 IgG and IgA titers) in longitudinally analyzed COVID-19 patient samples. Circle size and color represents the correlation coefficient and data is shown only for statistically significant ($p < 0.05$) correlations after Benjamini-Hochberg correction for multiple comparisons. **(B)** Correlation between D0 pNT_{50} and time to disease resolution. (Pearson's correlation coefficient r=-0.2194, p=0.0267). **(C)** pNT_{50} in outpatients who resolved disease within the first 7 days (n=48) after enrolment compared with those who had symptoms for 8 or more days (n=57).

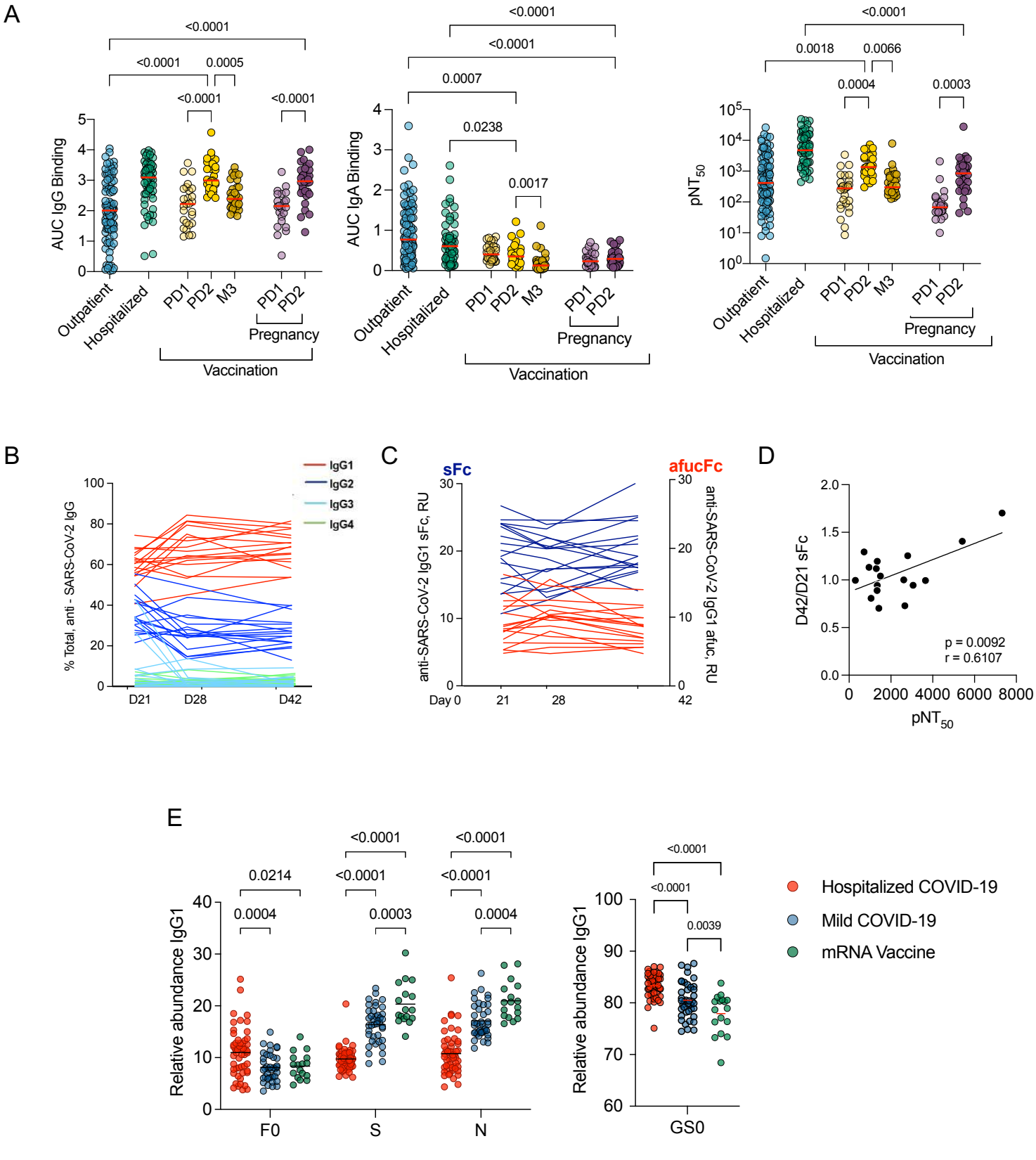

Figure 5. mRNA vaccination elicits high neutralizing antibody titers with Fc glycoforms distinct from both infection-induced phenotypes. (A) SARS-CoV-2 full length spike (S) binding IgG (AUC), IgA (AUC) and half-maximal SARS-CoV-2 pseudovirus neutralizing titers (pNT_{50}) following mRNA vaccination in two independent cohorts comprising; healthy adults (yellow n=29) and pregnant women (purple n=28) and COVID-19 hospitalized patients (n=59) and outpatients (n=92) The median values have been depicted with a red line. PD1: post-dose 1 (day 21), PD2: post-dose 2 (day 42), M3: month 3. Longitudinal analysis of **(B)** IgG subclasses and **(C)** anti-SARS-CoV-2 IgG1 Fc afucosylation (afucFc) and sialylation (sFc) post-primary vaccination (day 21/D21), 7 days post boost (day 28/D28) and 3 weeks post-boost (day 42/D42) (n=17). **(D)** Correlation between D42 half-maximal neutralizing titers and fold change in levels of IgG1 Fc sialylation at D21 and D42 (Pearson correlation coefficient r=0.6107, p=0.0092). **(E)** SARS-CoV2 IgG1 Fc posttranslational modifications in hospitalized COVID-19 patients (n=52), COVID-19 outpatients (n=40) and mRNA vaccinees (n=17). F0: afucosylation, S: sialylation, N: bisection, GS0: galactosylation. P values (A) were calculated using Kruskal Wallis test with Dunn's correction and (E) with two-way ANOVA with Tukey's correction.

Extended Data Figure 1

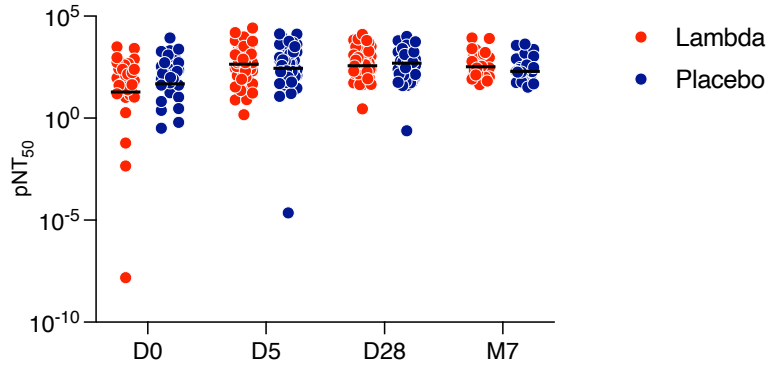

No impact of lambda treatment on neutralizing antibody titers. The pNT50 of patients treated with lambda (red) or placebo (purple) at enrollment day 0, 5, 28 and M7.

Extended Data Figure 2

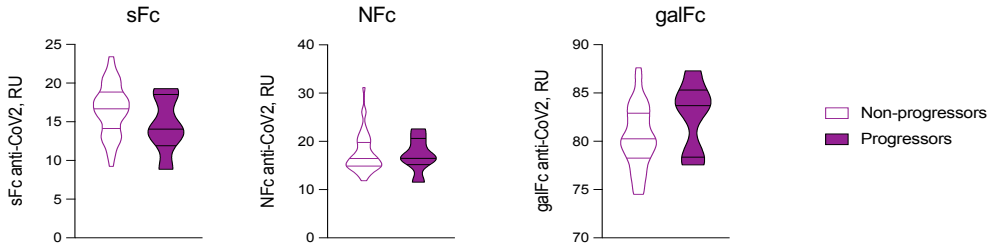

Anti-SARS-CoV-2 IgG1 Fc post-translational modifications. Sialylation (sFc), bisection (NFc) and galactosylation (galFc) levels in progressors and non-progressors.

Extended Data Figure 3

A

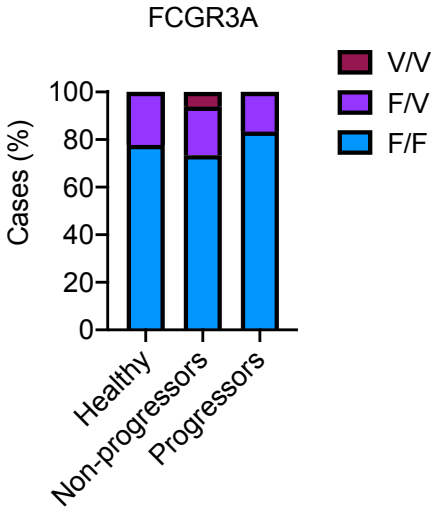

B

	F/F	F/V	V/V
Healthy	7	2	0
Non-progressors	36	10	3
Progressors	5	1	0

Distribution of FCGR3A allelic variants. The genotypes were characterized by Sanger sequencing, following PCR amplification of the FCGR3A genes using cDNA in progressors (n=6 available), non-progressors (n=49) and healthy controls (n=9). **(A)** Distribution of FCGR3A F/F, F/V and V/V variants among the subgroups. **(B)** Table showing the frequency of the FCGR3A F/F, F/V and V/V variants among the subgroups. There are no statistically significant differences among FCGR3A variants between non-progressors and progressors as determined by Fisher's exact test.

Extended Data Figure 4

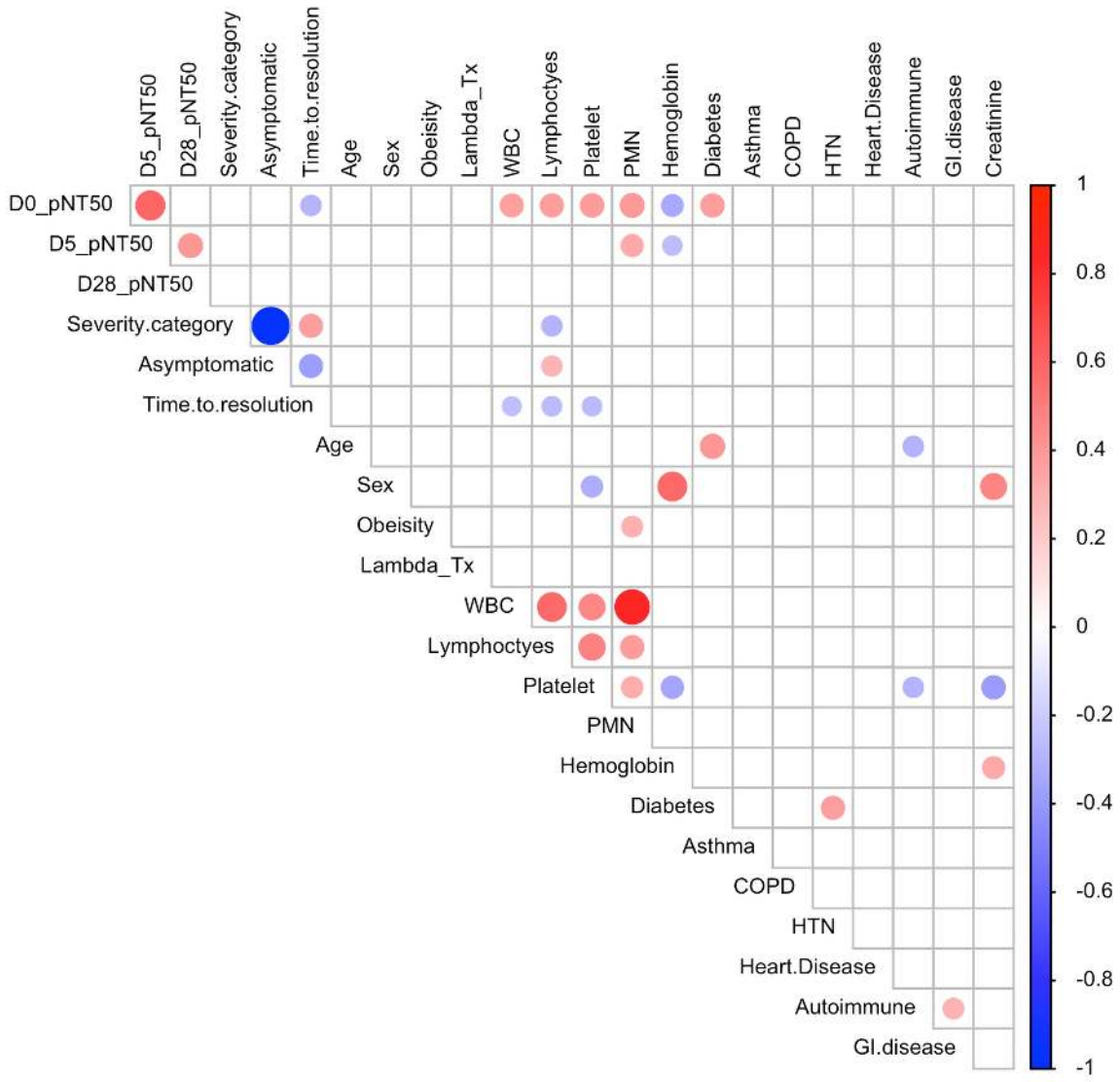

Clinical correlation matrix. The cross-correlation matrix shows the inter-relationship between the antibody neutralization titers in COVID-19 patient samples analyzed longitudinally with multiple immune parameters, disease severity and symptom duration. COVID-19 disease resolved earlier in patients with high neutralization titers at enrollment. Data is shown only for statistically significant ($p<0.05$) Spearman correlation coefficients after Benjamini-Hochberg correction for multiple comparisons. A multi-level assignment was used for each categorical variable to compute the spearman correlation. The assigned levels are listed here: Response (high = 1, low = 0), disease severity (asymptomatic = 0, moderate = 1, severe = 2), severe (no = 0, yes = 1), asymptomatic (no = 0, yes = 1), sex (female = 0, male = 1), obesity (no = 0, yes = 1), and interferon-lambda treatment (no = 0, yes = 1). The size and color of each circle correspond to the pair-wise correlation coefficient.

Extended Data Figure 5

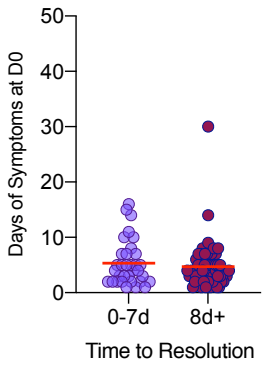

Symptom duration prior to enrollment. The duration of symptoms prior to enrolment in study participants who had an early resolution of disease (0-7days) as compared to those who had a longer course of disease (8d+). The p value in (C) was calculated using Mann Whitney unpaired t-test.

Extended Data Figure 6

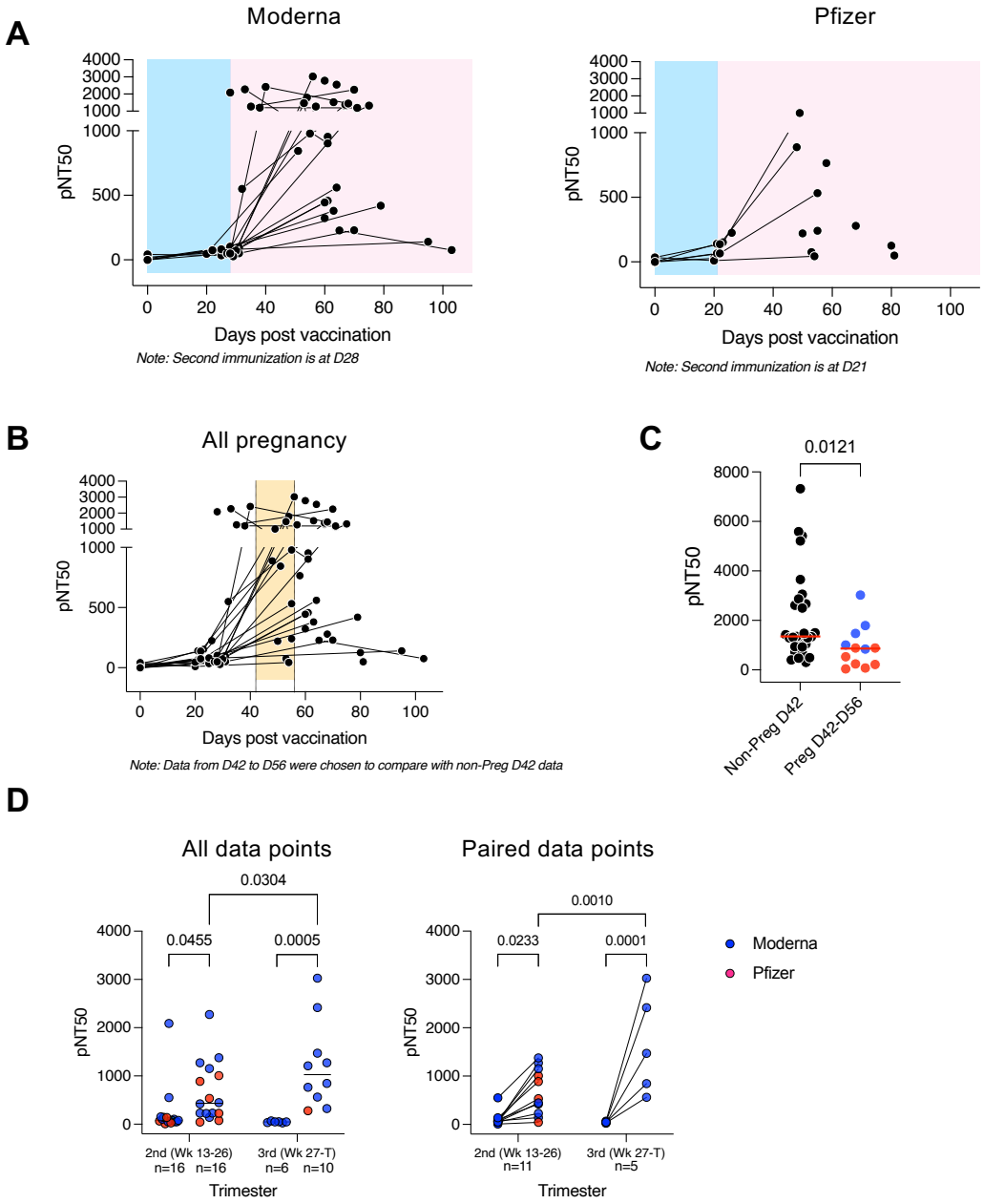

Pregnant mRNA vaccine cohort. (A) The neutralizing titers pNT_{50} for plasma obtained from pregnant women who had received the Moderna SARS-CoV-2 vaccine or the Pfizer SARS-CoV-2 vaccine. The pNT_{50} were determined through SARS-CoV-2 pseudovirus neutralization assays. The first immunization was delivered at day 0 for both vaccine cohorts. The second immunization was delivered at day 28 for the Moderna vaccine cohort and at day 21 for the Pfizer vaccine cohort. **(B)** Neutralization titers of all vaccinated pregnant patients. Data from both vaccine cohorts were plotted on the same graph. **(C)** Data from D42 to D56 (n=12) in (**B**), highlighted in yellow, were chosen to compare with non-Preg D42 data (n=31). A comparison between pNT_{50} values from non-pregnant vaccinated individuals at day 42 and pregnant vaccinated individuals at day 42 to 56. Red data points indicate pregnant patients who received the Pfizer SARS-CoV-2 vaccine. Blue data points indicate pregnant patients who received the Moderna SARS-CoV-2 vaccine. **(D)** The pNT_{50} of all vaccinated pregnant patients separated by trimester in pregnancy (left panel). Paired pre- and post-boost pNT_{50} analysis were also performed from patients with available data (right panel). N numbers are on the graph. Red data points indicate pregnant patients who received the Pfizer SARS-CoV-2 vaccine. Blue data points indicate pregnant patients who received the Moderna SARS-CoV-2 vaccine.

Extended Data Figure 7

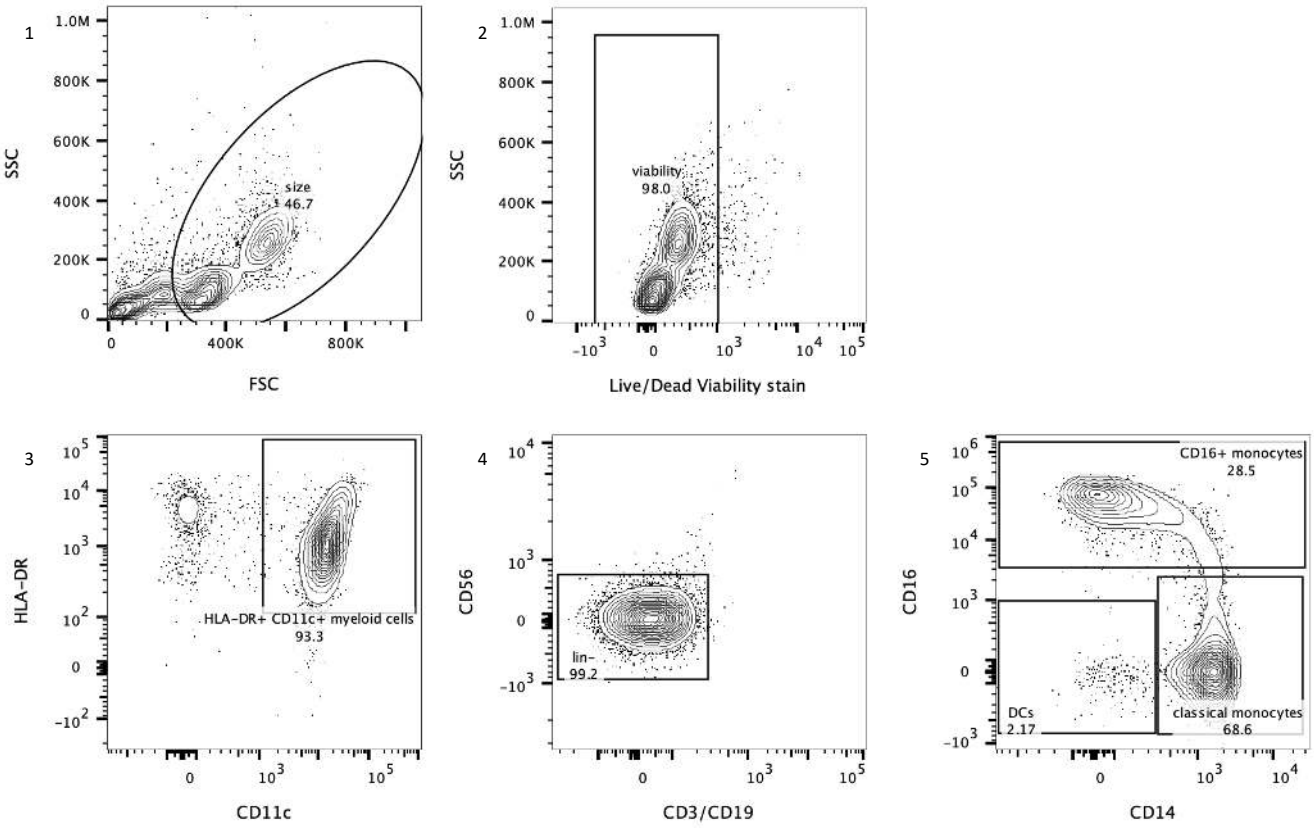

Gating strategy for bulk myeloid and CD16a+ cells. Bulk myeloid cells were defined as viable CD3- CD19- CD56- CD11c+ HLA-DR+ cells, while CD16a+ monocytes within this population were additionally positive for CD16a

Extended Data Figure 8

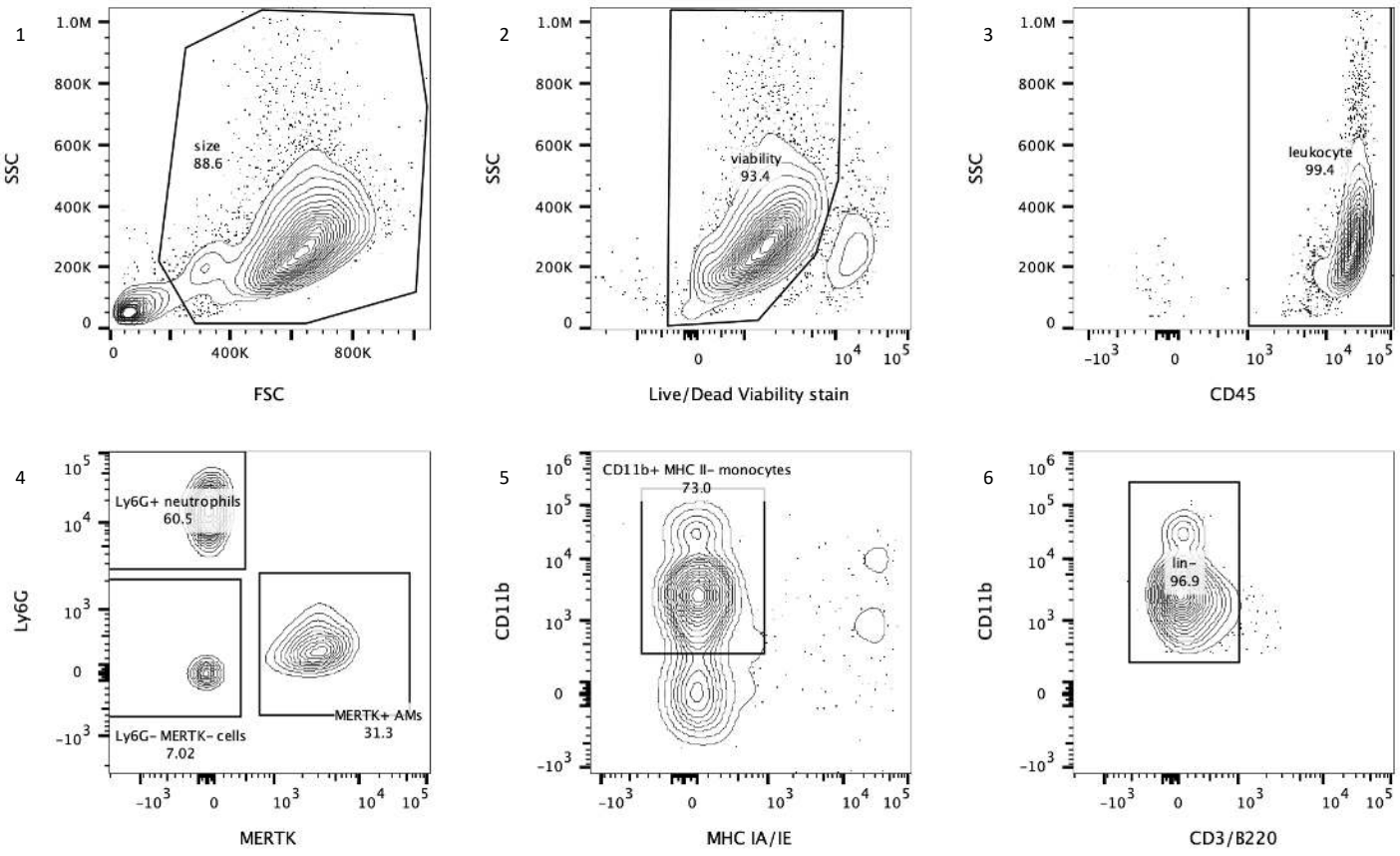

Gating strategy for immune cell infiltrates in mouse BAL. Neutrophils were defined as viable Ly6G+ CD11b+ CD3- B220- leukocytes. Monocytes were defined as viable CD11b+ Ly6G- MERTK- MHC IA/IE- CD3- B220- leukocytes.